

Finite-temperature behavior of the Anderson lattice

B. H. Brandow

Theoretical Division, Los Alamos National Laboratory, Los Alamos, New Mexico 87545

(Received 9 March 1987)

At finite temperature the picture of renormalized-hybridization quasiparticle bands, obtained by various formalisms at $T=0$, is shown to be inadequate in several respects. The most significant refinement recognizes the existence of a new type of elementary excitation, which simply creates (i.e., unbinds or unscreens) a local moment at an arbitrary lattice site. These excitations explain the continuous crossover between the contrasting $T \ll T_K$ and $T \gg T_K$ behaviors. They also explain the surprisingly rapid weakening, with increasing T , of inelastic peaks in neutron scattering. The concept of "coherence" is clarified. Numerical results are presented for entropy, specific heat, average valence, magnetic susceptibility, and inelastic neutron scattering.

I. INTRODUCTION

The Anderson lattice is widely accepted as a model for the basic electronic properties of valence-fluctuation materials, namely the family of mixed-valent, Kondo-lattice, and heavy-fermion materials. However, progress in solving this model has been rather limited.¹

Here we only consider the "normal" state, in the sense of Fermi-liquid theory, i.e., without magnetic order or superconductivity. It is well known experimentally that there is a smooth crossover, characterized by a temperature T_K (generally only loosely defined), such that the behaviors at $T \ll T_K$ and $T \gg T_K$ are strikingly different. In the "coherent" regime below T_K , several materials have provided clear evidence for a sharp Fermi surface or, alternatively, for a narrow insulating gap. This evidence demonstrates that the correct low- T description must be that of a *periodic* Fermi liquid, as described by Luttinger.² Several formal approaches have now provided some justification for this Luttinger (effective band structure) aspect.¹ The most detailed treatment of this aspect is our variational theory (Ref. 3, denoted hereafter as I), where extensive references are given.⁴ At the other extreme, $T \gg T_K$, high-temperature perturbation theory has shown conclusively that to leading order in $\beta = (k_B T)^{-1}$, one finds local moments which interact with each other only via the chemical potential.⁵ This justifies the high- T picture deduced from experiments.

A major problem has been the lack of a theory, and the corresponding lack of a clear conceptual picture, for the continuous crossover characterized by T_K . For example, previous efforts to extend the above-mentioned zero or very-low-temperature theories to higher T have led to an unphysical second-order phase transition.^{6,7} A number of other finite-temperature studies have been reported, but none of these are fully satisfactory either. The methods include: (a) Green's-function treatments where the f -electron self-energy is taken from the solution for a single impurity.⁸ This approach is clearly somewhat phenomenological. (b) The Hubbard I type of Green's-function approximation.⁹ This fails to satisfy

the Luttinger sum rule, and thereby locates the Fermi level incorrectly.¹⁰ It also has a strong preference for magnetic states,^{7,9} which seems to be unphysical. (c) Use of the alloy analogy, via the coherent potential approximation¹¹ (CPA). This incorporates alloy-disorder-type scattering even at $T=0$, and it thereby degrades the coherence which is known to exist at very low temperature. The resulting disorder broadening of the quasiparticle energies leads to spurious narrowing, and possible closure, of the hybridization gap. Nevertheless, this has probably been the most successful finite- T approach to date. (d) More refined self-consistent Green's-function treatments.¹² This program is ambitious and may eventually succeed, but it has so far provided little physical detail. In addition to these formal efforts, there are also several phenomenological models.¹³⁻¹⁶

We shall now demonstrate that, with suitable refinements, the variational formalism of I provides a clear picture of the basic crossover mechanism, and fixes its temperature scale unambiguously. The results also shed light on some characteristic low-temperature structures in specific heat, magnetic susceptibility, and inelastic neutron scattering. The basic theory is presented in Sec. II, and Sec. III presents thermodynamic results for both the heavy-fermion and mixed-valent regimes. This approximate theory is not entirely satisfactory, and Sec. IV discusses its deficiencies. Section V presents calculations of inelastic neutron scattering, and attempts to demonstrate that the present theory can explain the very strong temperature dependence of inelastic structures seen in a number of materials. Section VI outlines the implications of this theory for resistivity, and further discussion of the physical picture is presented in Sec. VII. The discussions in Secs. VI and VII provide a clear picture for the previously vague concept of "coherence."

II. FINITE-TEMPERATURE THEORY

For consistency with I, we use the orbitally nondegenerate Anderson-lattice Hamiltonian in the form

$$H = \sum_{k,\sigma} \varepsilon_k \hat{n}_{k\sigma} + \varepsilon_f \sum_{j,\sigma} \hat{n}_{j\sigma} + U \sum_j (1 - \hat{n}_{j\uparrow})(1 - \hat{n}_{j\downarrow}) + \sum_{k,j,\sigma} (v_{kj} \eta_{k\sigma}^\dagger \eta_{j\sigma} + \text{H.c.}), \quad (1)$$

where j is a site index, $\hat{n}_\alpha = \eta_\alpha^\dagger \eta_\alpha$, and we assume $U \rightarrow \infty$. This version describes fluctuations between local f^1 (magnetic) and f^2 (closed shell, nonmagnetic) configurations, as appropriate for Sm and Yb compounds. It is the particle-hole analog of the more common (Ce-type) form. The ground-state variational wave function is

$$\Psi = \prod_j \left[1 + \sum_{k,\sigma} a_{kj} \eta_{k\sigma}^\dagger \eta_{j\sigma} \right] | \Phi_c \Phi_f \rangle, \quad (2)$$

where Φ_c is a simple Fermi sea with conduction (k, σ) orbitals occupied for $k \leq k_F$, and Φ_f indicates that all $2N$ of the f orbitals are fully occupied,

$$\Phi_f = \left[\prod_j \eta_{j\uparrow}^\dagger \eta_{j\downarrow}^\dagger \right] | \text{vacuum} \rangle = \left[\prod_k \eta_{fk\uparrow}^\dagger \eta_{fk\downarrow}^\dagger \right] | \text{vacuum} \rangle. \quad (3)$$

(N is the number of lattice sites.) In the wave function (2) every site has spin-singlet character, corresponding to a bound or fully screened local moment.

At finite temperature, the resulting variational energy is

$$\langle H \rangle = \sum_{k,\sigma} \varepsilon_k f_{k\sigma}^+ + \sum_{k,\sigma} \frac{(\varepsilon_k - \varepsilon_f) A_k^2 + 2V_k A_k}{\mathcal{D}_b / c_b + A_k^2} (1 - f_{k\sigma}^+), \quad (4)$$

where

$$\frac{1}{\mathcal{D}_b} = 1 - \frac{1}{Nc_b} \sum_{k,\sigma} \frac{A_k^2}{\mathcal{D}_b / c_b + A_k^2} (1 - f_{k\sigma}^+) = 1 - \xi_b, \quad (5)$$

$$a_{kj} = N^{-1/2} A_k \exp(-ik \cdot R_j), \quad (6)$$

and V_k is related to v_{kj} in the same manner. Also, $f_{k\sigma}^+ = f(\mathcal{E}_{k\sigma}^+ - \zeta)$ is the Fermi function for the upper branch of the quasiparticle spectrum (see below), the branch that intersects the Fermi level ε_F (or chemical potential ζ). (We assume $n_e \geq 2$, where n_e is the number of electrons per site.) The "new" parameter c_b is the concentration of bound (screened or quenched local-moment) sites, as discussed below. \mathcal{D}_b is the normalization factor for a bound site, and ξ_b is the f^1 probability for this site. The total number of electrons transferred virtually from f orbitals to conduction orbitals by means of hybridization (the v_{kj} 's) is $Nc_b \xi_b$, and the overall f^1 probability (the valence parameter), averaged over all sites, is

$$\xi = c_b \xi_b + (1 - c_b). \quad (7)$$

At the present level of approximation, based on (2), the unbound (local-moment) sites are totally nonhybridizing. Corrections to this simple picture are outlined below and in Secs. V–VII.

For $T=0$, where $c_b=1$ and $f_{k\sigma}^+$ is merely a step function, the basic expressions (4) and (5) have been obtained

from an elementary physical argument³ and, independently, by means of a diagrammatic analysis.¹⁷ The manner of occurrence of c_b in (4) and (5) was also discussed in I (see the Appendix), where this parameter was called P_2^0 . The occurrence of the $f_{k\sigma}^+$'s at $T \neq 0$ is an obvious extension. From Landau's original definition of the quasiparticle energy,¹⁸ we find that a quasiparticle in the upper branch has energy

$$\begin{aligned} \mathcal{E}_{k\sigma}^+ &\equiv \frac{\delta \langle H \rangle}{\delta f_{k\sigma}^+} = \frac{\partial \langle H \rangle}{\partial f_{k\sigma}^+} + \frac{\partial \langle H \rangle}{\partial \mathcal{D}_b} \frac{\delta \mathcal{D}_b}{\delta f_{k\sigma}^+} \\ &= \varepsilon_k - \frac{(\varepsilon_k - \varepsilon_f - \mu) A_k^2 + 2V_k A_k}{\mathcal{D}_b / c_b + A_k^2} \\ &= \varepsilon_k - \frac{V_k A_k}{\mathcal{D}_b / c_b}. \end{aligned} \quad (8)$$

All of the variational parameters A_k are optimized by the stationary condition

$$\frac{\delta \langle H \rangle}{\delta A_k} = \frac{\partial \langle H \rangle}{\partial A_k} + \frac{\partial \langle H \rangle}{\partial \mathcal{D}_b} \frac{\delta \mathcal{D}_b}{\delta A_k} = 0, \quad (9)$$

which leads to the quadratic expression

$$V_k A_k^2 - (\mathcal{D}_b / c_b) [(\varepsilon_k - \varepsilon_f - \mu) A_k + V_k] = 0. \quad (10)$$

We choose the solution that makes A_k positive, since for convenience we are assuming that V_k is negative. The optimization condition (10) was used in obtaining the final expression in (8).

The parameter μ , which arises from the $\delta \mathcal{D}_b / \delta A_k$ term in (9) [and from the $\delta \mathcal{D}_b / \delta f_{k\sigma}^+$ term in (8)], is found to be

$$\mu = \frac{\mathcal{D}_b}{N} \sum_{k,\sigma} \frac{V_k A_k}{\mathcal{D}_b + c_b A_k^2} (1 - f_{k\sigma}^+). \quad (11)$$

All of the above analysis is explained in I.

There are actually two branches in the quasiparticle spectrum, with energies

$$\mathcal{E}_{k\sigma}^\pm = \frac{1}{2} \{ \varepsilon_k + \bar{\varepsilon}_f \pm [(\varepsilon_k - \bar{\varepsilon}_f)^2 + 4\bar{V}_k^2]^{1/2} \}. \quad (12)$$

This has exactly the elementary-hybridization form obtained from (1) when $U=0$, except for the parameter renormalizations

$$\bar{\varepsilon}_f = \varepsilon_f + \mu, \quad (13)$$

$$\bar{V}_k = V_k [c_b (1 - \xi_b)]^{1/2}. \quad (14)$$

Thus we have an appealingly simple "renormalized hybridization" picture for the quasiparticles.^{3,4} Similar results for $\mathcal{E}_{k\sigma}^\pm$ have been obtained by others.^{4,6,19} However, we shall now argue that this simple result needs to be refined in *three* respects.

For an orientation, we look beyond the present level of approximation, based on (2), and briefly consider the more elaborate "two-parameter" approximation described in I. We noted there that spin-flip scattering (between conduction electrons and unbound local moments) is allowed in the latter version, consistent with one's expectation for a general theory. This leads us to envisage

the thermal excitation of \mathcal{E}^- states as involving two steps. First, an $\mathcal{E}_{k\sigma}^-$ state is excited. This involves replacing the Φ_f in (2) by

$$\eta_{fk\sigma}\Phi_f = N^{-1/2} \sum_j e^{-ik \cdot R_j} \eta_{j\sigma}\Phi_f, \quad (15)$$

an f^1 configuration distributed coherently over the entire lattice as a Bloch superposition. [This replacement is analogous to (8), which corresponds to varying the $k\sigma$ conduction-orbital occupation in Φ_c .] This state (15) is obviously different from the conventional picture of a local moment. The second step is a scattering event (possibly involving spin flip), which destroys the phase coherence and localizes the f^1 configuration at some site j , thereby producing an ordinary local moment. These two steps are, of course, merely a conceptual aid; the physical excitation process may well involve only a single step. We are thus led to conclude that there are actually three types of elementary excitations, namely $\mathcal{E}_{k\sigma}^+$ quasiparticles, $\mathcal{E}_{k\sigma}^-$ quasiparticles [retaining the phase coherence (15), with energy (12)], and the present local-moment or moment-unbinding excitations. This constitutes the *first* refinement.

The total energy cost for a moment-unbinding excitation is just $-\bar{\epsilon}_f$, according to an analysis in I.²⁰ The difference $-(\bar{\epsilon}_f - \epsilon_f) = -\mu$ is the loss of interaction energy due to unbinding one site. At finite T all $2N$ of the $k\sigma$ hybridization channels contribute to this energy change, although the low- ϵ_k contributions are strongly inhibited by the $1-f_{k\sigma}^+$ factors in (11). In the limit $c_b \rightarrow 0$, the expression (11) for μ becomes just the binding energy for a single impurity.²¹ A moment-unbinding excitation involves the removal of an electron, which must then be returned to the system, so the *net* excitation energy is $\zeta - \bar{\epsilon}_f$. The probability of finding a local moment (unbound or unscreened) at site j is now seen to be

$$P_{lm} = 2e^{-\beta(\zeta - \bar{\epsilon}_f)} / (1 + 2e^{-\beta(\zeta - \bar{\epsilon}_f)}), \quad (16)$$

where the factor 2 comes from spin degeneracy. It follows that the concentration of bound sites is

$$c_b = 1 - P_{lm}. \quad (17)$$

Noting the $\bar{\epsilon}_f$ is the midpoint of the gap [see (12)], we see that a typical thermal $\mathcal{E}_{k\sigma}^-$ excitation would expend, very roughly, about twice as much energy as a moment unbinding.²² The latter excitations must therefore be far more numerous at any finite temperature, and this leads us to neglect the probability of thermal $\mathcal{E}_{k\sigma}^-$ excitations. Viewed from a different perspective, we see that the $\mathcal{E}_{k\sigma}^-$ excitations are energetically unstable against decay into moment-unbinding excitations. Thus, for example, a wave packet of phonons could trigger the collapse of an $\mathcal{E}_{k\sigma}^-$ excitation into a localized moment unbinding. (In the same vein, an intersection of two phonon wave packets could directly create a moment unbinding.) A further argument for neglecting thermal $\mathcal{E}_{k\sigma}^-$ excitations is that, collectively, they duplicate the degrees of freedom described by the $2N$ possibilities for a moment-unbinding excitation. Finally, we note that the combined total number of $\mathcal{E}_{k\sigma}^-$ and moment-unbinding excitations can-

not exceed N , when $U = \infty$, in view of the effect of each one of these excitations in Φ_f . Therefore, moment-unbinding excitations not only must greatly outnumber $\mathcal{E}_{k\sigma}^-$ thermal excitations (and perhaps totally exclude them), they must also decrease the *availability* of $\mathcal{E}_{k\sigma}^-$ states for possible excitation, even by nonthermal (k -conserving) processes such as inelastic neutron scattering. The *second* refinement is this observation that there are kinematical constraints which reduce the probability of $\mathcal{E}_{k\sigma}^-$ excitations. [The corresponding constraint upon the moment-unbinding excitations, assuming no $\mathcal{E}_{k\sigma}^-$ excitations, is seen in the Boltzmann-statistics form of (16).] This constraint aspect will be used in Sec. V below, and further consequences will be discussed elsewhere.

The equations for the present approximate theory are completed as follows: The chemical potential ζ is determined by electron-number conservation,

$$n_e = 2 - P_{lm} + \frac{1}{N} \sum_{k,\sigma} f_{k\sigma}^+. \quad (18)$$

The entropy (per site) consists of two parts, an \mathcal{E}^+ part involving $f_{k\sigma}^+$'s in the usual Fermi-statistics manner,

$$S^+ = -\frac{k_B}{N} \sum_{k,\sigma} [f_{k\sigma}^+ \ln f_{k\sigma}^+ + (1 - f_{k\sigma}^+) \ln(1 - f_{k\sigma}^+)], \quad (19)$$

and a local-moment part,

$$S^- = -k_B \left[c_b \ln c_b + P_{lm} \ln \left[\frac{P_{lm}}{2} \right] \right], \quad (20)$$

involving Boltzmann statistics. The specific heat C is obtained by numerical differentiation of (4).

The static magnetic susceptibility (divided by $N\mu_B^2$) is the sum of (a) the $\omega=0$, $q \rightarrow 0$ limit of $\text{Re}\chi^0$, as discussed in Sec. V, and (b) a local-moment term,

$$\chi_{lm} = P_{lm} / k_B T. \quad (21)$$

Contribution (a) has the expected quasiparticle form,

$$\chi_{qp} = \frac{1}{N} \sum_{k,\sigma} \left[-\frac{\partial f_{k\sigma}^+}{\partial \mathcal{E}_{k\sigma}^+} \right], \quad (22)$$

which reduces to the quasiparticle state density, $\rho(\epsilon_F)$, as $T \rightarrow 0$.

III. THERMODYNAMIC RESULTS

Calculations were done by the Newton method, regarding $c_b \xi_b$, μ , ζ , and c_b as independent variables. Formally, of course, c_b is fully determined by μ , ζ , and ξ_b , but use of these three variables alone led to numerical instability at $T \ll T_K$, where P_{lm} is exceedingly small. The identity $dS/dT = C/T$ provided a useful check on numerical accuracy.

The results are shown in Figs. 1 and 2. These use the same basic parameters as in I—a rectangular conduction band of total width 2 eV, $V_k = -(0.05)^{1/2}$ eV, and $n_e = 2.4$. The parameter D_- (energy ϵ_f with respect to the bottom of the conduction band) is 1.65 eV in Fig. 1, giving at $T=0$ the results $\xi = 0.961$, $\mu = -0.288$ eV, and

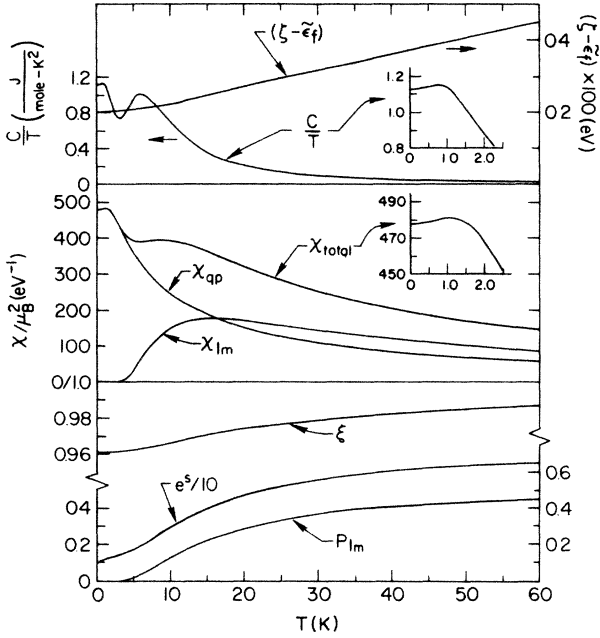


FIG. 1. Thermodynamic results for the heavy-firmion regime. See text for parameters used.

$\gamma = 1.13 \text{ J/mol K}^2$, typical of the heavy-firmion regime. Figure 2 shows the results for $D_- = 1.3 \text{ eV}$, the corresponding $T=0$ results being $\xi = 0.712$, $\mu = -0.191 \text{ eV}$, and $\gamma = 0.0893 \text{ J/mol K}^2$, typical of the mixed-valent regime.

In each case, C/T shows two peaks—a very-low- T peak due to the sharp spike in the $\mathcal{G}_{k\sigma}^+$ state density (at the bottom of this subband), and a higher- T peak due to moment-unbinding excitations. As discussed in I, the heavy-firmion materials provide ample evidence for both types of peaks. The magnitudes of these peak temperatures, and especially their ratios ($T_{\text{high}}/T_{\text{low}}$), are quite similar to the results in Fig. 1. The amplitude of the second C/T peak is, however, far too large compared to experiment. (Typically, there is only a mild peak in C , which becomes a nearly invisible shoulder in C/T .) As explained in Sec. IV, this feature is an artifact of our approximation.

The susceptibility results also show two features, a very-low- T peak followed by a higher- T peak or shoulder, at temperatures slightly higher than those of the corresponding C/T features. Such a very-low- T peak has been positively identified for only one heavy-firmion material [CeAl₃ (Ref. 23)], but a prominent kink in χ , in this temperature range, may be seen in the data for several other materials. As in the case of C/T , the prominence of the higher- T feature (peak or shoulder) in χ is an artifact of our approximation, as explained in Sec. IV. Turning to the mixed-valent case, we note that there is one material (CePd₃) for which there is now strong evidence that the observed “low- T upturn” in χ is intrinsic,²⁴ consistent with the very-low- T peak in Fig. 2. In fact, there is also some CePd₃ data that show a clear low- T peak of the present form.²⁵

Overall, these results show remarkably little difference

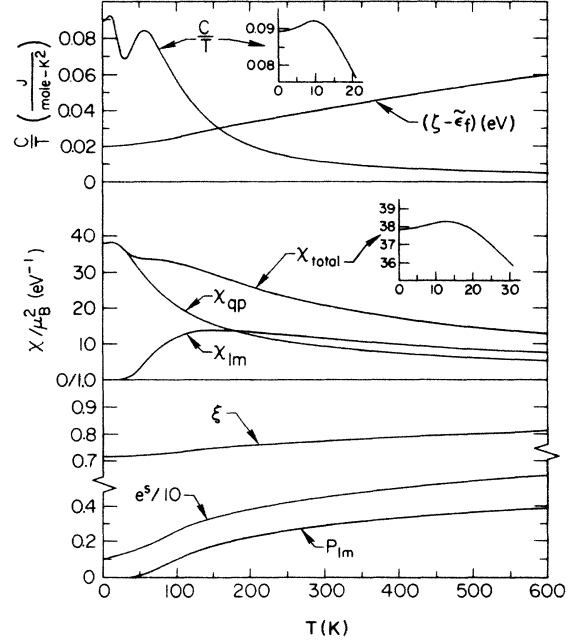


FIG. 2. Thermodynamic results for the mixed-valent regime. See text for parameters used.

between the heavy-firmion and mixed-valent regimes. Experimentally, however, the higher- T feature in χ becomes far more conspicuous for materials in the mixed-valent regime. There is a simple reason for this. The larger temperature scale leads to crystal-field excitations. This increases the effective magnetic moment, and thereby strongly enhances the χ_{lm} contribution.

IV. CRITIQUE OF THE APPROXIMATION

There is a seriously unsatisfactory feature in the present treatment. The basic formulas, (4) and (5), involve a virtual-crystal approximation: each site is assumed to be hybridizing with fractional strength c_b , so that full translational invariance is maintained. The result is that, even at $T \gg T_K$, the \mathcal{G}^+ spectrum retains the form (12) and, therefore, has an extensive flat region with $\mathcal{G}_{k\sigma}^+$'s close to $\bar{\epsilon}_f$. Ideally, what should be done is to calculate with a number Nc_b of bound (hybridizing) sites fixed on some array, and then average the results (especially for $\mathcal{G}_{k\sigma}^+$ and $\bar{\epsilon}_f$) over all such spatial arrangements. This is the *third* needed refinement. We have not yet implemented this, but we mention that a few results are known: With *no* bound sites ($c_b = 0$), $\mathcal{G}_{k\sigma}^+$ reduces to the bare ϵ_k spectrum, and with just one bound site ($c_b = N^{-1}$), $\mathcal{G}_{k\sigma}^+ - \epsilon_k$ is $O(N^{-1})$.²⁶ The case of just one local moment ($c_b = 1 - N^{-1}$) can also be treated without the virtual-crystal approximation.⁷ (This exercise confirms that the moment-unbinding energy is close to $\zeta - \bar{\epsilon}_f$, as obtained in the present periodic approximation.) In view of these solvable cases, an improved treatment of the $\mathcal{G}_{k\sigma}^+$ spectrum (and $\bar{\epsilon}_f$) should certainly be feasible.

The obvious conclusion to be drawn from these solvable cases is that, near the energy ζ , the $\mathcal{G}_{k\sigma}^+$ state densi-

ty (i.e., the effective mass) must be rapidly diminishing as P_{lm} increases, in contrast to the present approximation. It is, therefore, clear that when the S^- contribution (20) is increasing rapidly, the corresponding S^+ contribution (19) must be increasing far less rapidly than in the present calculations. There may even be a temperature range over which S^+ decreases with increasing T , but, of course, it can only do so more slowly than the increase of S^- . The present treatment therefore grossly overestimates the S^+ entropy contribution at $T \gtrsim T_K$, and likewise for the amplitude of the second C/T peak. For the same reason, our χ_{qp} is also too large at $T \gtrsim T_K$, and correcting this must diminish the second peak (or shoulder) in χ .

By setting $c_b = 0$ and $A_k = V_k / (\bar{\epsilon}_f - \epsilon_k)$ in (11) we obtain the corresponding single-impurity result, in which μ is given by a digamma-function expression.²⁷ This suggests that with an improved treatment, at $T \gg T_K$, $|\mu|$ may become much smaller than its $T=0$ value. This would mean that in the Kondo or heavy-fermion regime (ϵ_f lying high in the conduction band³), where $|\mu|$ can be $\gg k_B T_K$ at $T=0$, there could be a temperature range $T_K < T < (\epsilon_f - \zeta) / k_B$ in which $P_{lm} \approx 1$ and $S \approx \ln 2$ (local-moment regime), followed at higher temperatures, $T \gtrsim (\epsilon_f - \zeta) / k_B$, by an entropy-limit regime with $P_{lm} \approx \frac{2}{3}$ and $S \approx \ln 3$. This type of crossover is known to occur for a single Anderson impurity,²⁸ and it may therefore be expected for the lattice, in view of the high- T perturbation result.⁵ On the other hand, (18) forces ζ to rise considerably as the moments become unbound; thus, a careful analysis is required here. In any event we expect the rise of P_{lm} to be steeper, and to continue to higher values of P_{lm} , than in the present approximation.

V. INELASTIC NEUTRON SCATTERING

The present results have important consequences for inelastic neutron scattering. This scattering is proportional to $\text{Im}\chi(q, \omega)$, where, in the present picture, the dynamical susceptibility has the random-phase-approximation (RPA) form $\chi = \chi^0 / (1 + \mathcal{J}\chi^0)$, and \mathcal{J} is a quasiparticle interaction with suitable indices. This \mathcal{J} has not been adequately explored, and is therefore ignored here. As others have pointed out,²⁹⁻³² χ^0 consists of an intraband contribution and an interband contribution, denoted here as χ_{++}^0 and χ_{-+}^0 , respectively. In the present theory, these are

$$\chi_{++}^0(q, \omega) = \frac{1}{N} \sum_{k, \sigma} \frac{P_{fk\sigma}^+ P_{f, k+q, \sigma}^+ (f_{k\sigma}^+ - f_{k+q, \sigma}^+)}{\mathcal{E}_{k+q, \sigma}^+ - \mathcal{E}_{k\sigma}^+ - \omega - i\delta}, \quad (23)$$

$$\chi_{-+}^0(q, \omega) = \frac{c_b}{N} \sum_{k, \sigma} \frac{P_{fk\sigma}^- P_{f, k+q, \sigma}^+ (1 - f_{k+q, \sigma}^+)}{\mathcal{E}_{k+q, \sigma}^+ - \mathcal{E}_{k\sigma}^- - \omega - i\delta}. \quad (24)$$

Our χ_{++}^0 has a standard Fermi-liquid form, except that each quasiparticle is weighted by its f probability (fractional f content) $P_{fk\sigma}^+$, as described in I. (This determines the fraction of the scattering that follows the f -electron form factor; see below.) The χ_{-+}^0 expression is similar, but is reduced by the factor c_b . This factor

arises because each $\mathcal{E}_{k\sigma}^-$ state has probability c_b of being available for excitation (the "second refinement" in Sec. II). For completeness, we mention that χ^0 also includes a similar term,

$$\chi_{+-}^0(q, \omega) = \frac{c_b}{N} \sum_{k, \sigma} \frac{P_{f, k+q, \sigma}^- P_{fk\sigma}^+ (f_{k\sigma}^+ - 1)}{\mathcal{E}_{k+q, \sigma}^- - \mathcal{E}_{k\sigma}^+ - \omega - i\delta}, \quad (25)$$

but its imaginary part contributes only to neutron-energy-gain scattering.

In taking the $\omega=0, q \rightarrow 0$ limit of $\text{Re}\chi^0$, to obtain the static susceptibility of Sec. II, it must be remembered that each of these $\chi_{\mu\nu}^0$ expressions should actually contain a matrix-element factor of the form³³

$$|\langle \psi_{k+q, \sigma}^{\nu} | e^{iq \cdot r} | \psi_{k\sigma}^{\mu} \rangle|^2.$$

This leads to the familiar factor $|F(q)|^2$, where $F(q)$ is the f -electron form factor. It also gives the P_f factors included above. [Unlike the above $\chi_{\mu\nu}^0$ expressions, this $F(q)$ is not periodic in the extended-zone representation of k space.] In the $q \rightarrow 0$ limit of χ_{++}^0 , however, the complete matrix-element factor becomes unity (with conduction-orbital contributions now included); thus, we have deleted the P_f factors in obtaining the χ_{qp} result (22). In contrast, for the interband terms χ_{-+}^0 and χ_{+-}^0 the complete matrix-element factor vanishes as $q \rightarrow 0$.^{34(a)} These observations are essential for obtaining the correct static susceptibility expression (22), as is well known in conventional band theory.^{33, 34(a)} Nevertheless, for the calculations in this section we retain only the P_f -factor part of these matrix-element factors. The corresponding d -orbital or conduction-orbital scattering contribution is very small in the energy range of interest here, regardless of q , because its effective state density is distributed over a wide energy range corresponding to the "bare" bandwidth W ; see Eq. (44) of I. In a realistic system there is also a Van Vleck contribution to the static χ , and a corresponding finite-energy absorption due to crystal-field excitations. These can be incorporated within the present framework.^{34(a)}

Obviously, $\text{Im}\chi_{-+}^0$ is strongly inelastic, i.e., it has an inelastic threshold, in contrast to $\text{Im}\chi_{++}^0$. It is also very plausible that $\text{Im}\chi_{-+}^0$ should be strongly peaked at the q which spans the indirect gap between the \mathcal{E}^- and \mathcal{E}^+ branches, in other words, at a zone boundary, even when ϵ_F is not in the gap. (This can be seen by using an extended-zone representation to examine the phase space for the k integration.) This is certainly to be expected for three-dimensional lattices, and this has been confirmed for fcc (Ref. 29) and simple-cubic (Refs. 30 and 32) models. This is obviously untrue, however, for the one-dimensional case,^{34(b)} unless $n_e = 2.0$ so that the Fermi level falls in the gap. The two-dimensional model discussed below is an intermediate case, as we shall see. A true gap between the \mathcal{E}^+ and \mathcal{E}^- subbands is not essential for this q -dependent inelastic peak; even a pseudogap will suffice, as demonstrated in Ref. 32. (A pseudogap may result when a more realistic V_k is used, or when considering several conduction bands ϵ_k .)

We now want to emphasize that the strong tempera-

ture dependence of c_b must decrease χ_{-+}^0 with increasing T , at a rate that is rapid compared to the peak energy of this inelastic term. This is because the activation energy $\xi - \bar{\epsilon}_f$ is considerably less (by, very roughly, a factor of 2) than the energy of this inelastic peak.²² A great rapidity of “inelastic” temperature dependence has been noted experimentally, for several materials, but this has not previously been explained adequately.

These special “inelastic” features (peaking of the intensity at q equal to the zone boundary, and/or its surprisingly rapid decrease with increasing T) have now been observed in a number of materials: TmSe (Ref. 35), CeSn₃ and YbCuAl (Ref. 36), YbAl₃ (Ref. 37), CePd₃ and α -Ce (Ref. 38), CeCu₆ (Ref. 39), UPt₃ (Ref. 40), and even for the magnetic materials URu₂Si₂ (Ref. 41) and U₂Zn₁₇ (Ref. 42). In the latter materials, the magnetic order below T_N produced only minor changes in the “inelastic” scattering.

In Figs. 3 and 4 we present the results for a square-lattice tight-binding model. This model has its conduction-band limits, V_k , and ϵ_f position coinciding with the model for Fig. 1, and the finite- T values of ξ_b , μ , ζ , and c_b are taken from the Fig. 1 calculation. Although not fully self-consistent, this model should be adequate for our present purposes. The calculations were done directly from (23) and (24), using complex arithmetic, and taking $\delta = 1.5$ K. Figure 3 shows results for $\mathbf{q} = (q, q)$, the reduced q ranging from 0 to 1, and Fig. 4 shows the corresponding results for $\mathbf{q} = (q, 0)$. The re-

sults shown are for the dynamical structure factor $S(q, \omega)$, namely $\text{Im}\chi^0$ multiplied by the Bose factor

$$[1 - \exp(-\omega/T)]^{-1}.$$

This $S(q, \omega)$ is essentially the differential scattering intensity. The contributions from χ_{++}^0 and χ_{-+}^0 are shown separately, as the left- and right-hand curves, respectively. We first discuss the very-low-temperature ($T \ll T_k$) behavior, the solid-line curves for $T = 2$ K, noting that the $T = 0$ value of $\xi - \bar{\epsilon}_f$ is 23.5 K here. (We are now expressing all energies as temperatures.)

In Fig. 3, for $\mathbf{q} = (q, q)$, the “quasielastic” contribution from χ_{++}^0 is seen to have a Lorentzian-like form. ($\text{Im}\chi_{++}^0$ is close to the “ $\omega \times$ Lorentzian” form commonly employed in the neutron data analyses.⁴³) Its width increases rapidly with q , and its intensity rapidly diminishes for $q > 0.6$. The “inelastic” contribution from χ_{-+}^0 has a threshold ω which decreases with increasing q . Its maximum intensity is found for $q \sim 0.5$, and likewise for the magnitude of its prominent step-like onset. However, the relative importance of χ_{-+}^0 is greatest at $q = 1.0$, where the corresponding χ_{++}^0 contribution is unobservably small.

The qualitative features of Fig. 4, for $\mathbf{q} = (q, 0)$, are rather different. The χ_{++}^0 intensity remains strong at large q , and it also acquires a secondary peak at $q \gtrsim 0.5$. The χ_{-+}^0 threshold ω is considerably larger than in Fig. 3, but it likewise decreases with increasing q . The inten-

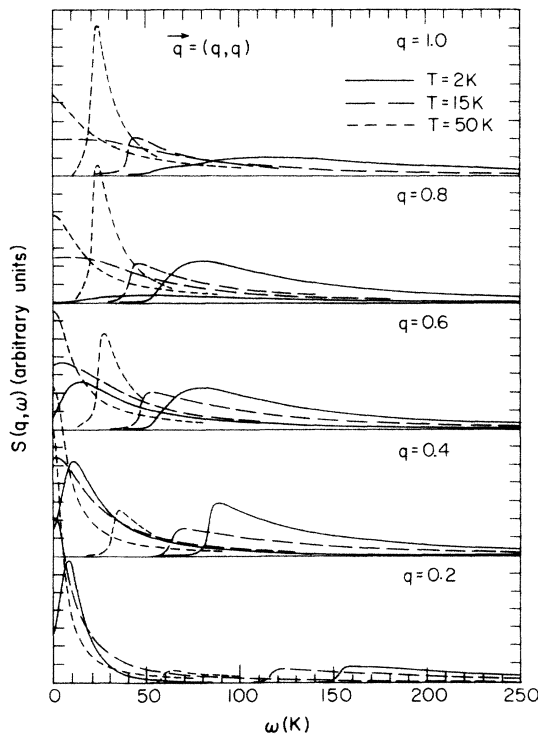


FIG. 3. $S(\mathbf{q}, \omega)$ for square-lattice model, $\mathbf{q} = (q, q)$. Arbitrary units. Parameters similar to those of Fig. 1, as described in text. The contributions from χ_{++}^0 and χ_{-+}^0 are shown separately, as the left- and right-hand curves, respectively.

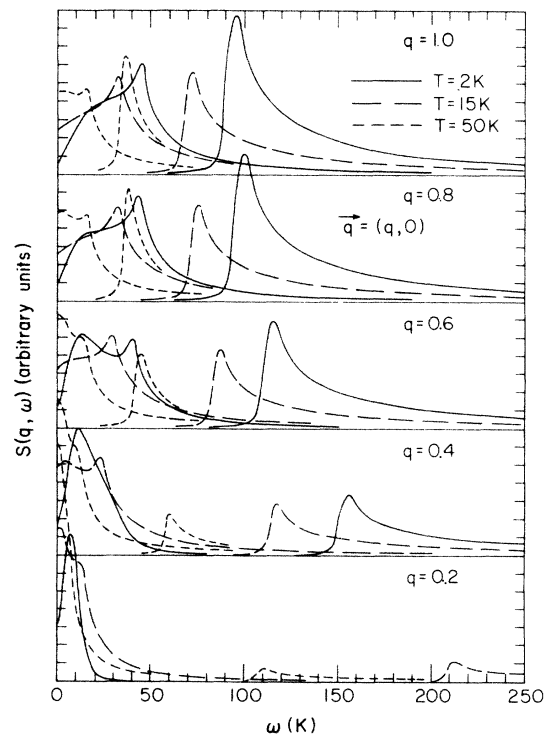


FIG. 4. $S(\mathbf{q}, \omega)$ for $\mathbf{q} = (q, 0)$. Units and model parameters are the same as in Fig. 3.

sity and threshold step height both increase steadily with q , and both peak at the zone boundary. The secondary χ_{++}^0 peak and the very strong χ_{-+}^0 peak both result from the saddle in ϵ_k at k_x equal to the zone boundary, $k_y=0$, and from the ridge and valley for finite k_y , along this k_x zone boundary and $k_x=0$, respectively. The contrasts between Figs. 3 and 4 hint at the complexity to be expected for more realistic band structures. (Compare with Ref. 29.) In a powder-pattern experiment, the "inelastic" structure should be dominated by the zone-boundary peak of Fig. 4. Note also that the energy of this peak is considerably greater than the true onset of χ_{-+}^0 intensity, which is seen in Fig. 3 (solid curve for $q=1.0$) to be at about 50 K.

The strong peaking of inelastic intensity at the zone boundary has previously been referred to as an antiferromagnetic tendency, and this has recently been attributed to a Ruderman-Kittel-Kasuya-Yosida (RKKY) interaction.³⁹ It should now be clear that *neither* of these interpretations is correct. The structures seen in Figs. 3 and 4 are merely a reflection of the $U=0$ hybridized band structure, while the effect of U here (at $T \ll T_K$) is simply to provide the renormalizations (13) and (14), with the latter reducing the overall energy scale. This view is also confirmed by calculations of the $T=0$ static structure factor $S(q)$.⁴⁴ In fact, it is known that related correlations exist even in a simple tight-binding metal,^{45,46} although these correspond only to our "quasielastic" (χ_{++}^0) results. The present large- q "inelastic" correlations are due specifically to the hybridization V_k , as shown here and in Ref. 44. One must conclude that this q dependence is not at all diagnostic for the presence of an antiferromagnetic interaction.

This is certainly not a denial that quasiparticle and RKKY interactions exist, or that these interactions may stabilize a magnetic ground state. The point is, rather, that proper identification of the effects of such interactions, in inelastic neutron scattering, requires more careful analysis than has previously been recognized. It is also worth noting that, because the $\mathcal{E}_{k\sigma}^{\pm}$ quasiparticles are admixtures of f (moment-producing) orbitals and conduction (RKKY coupling) orbitals, the RKKY interaction is not distinct from the quasiparticle interaction. The RKKY interaction is merely one aspect of the quasiparticle interaction, an aspect that becomes apparent only when some local magnetization is present.

We turn now to the temperature dependence in Figs. 3 and 4. The rapid decrease of the "inelastic" (χ_{-+}^0) thresholds is probably a consequence of our virtual-crystal approximation, as discussed in Sec. IV. The energy scale for *all* of the $S(q, \omega)$ features is renormalized here by $\bar{V}_k^2/V_k^2=c_b(1-\xi_b)$. However, in an improved treatment we expect the bound-state aspects to renormalize only as $1-\xi_b$, at least when c_b is small, since this is the behavior of the corresponding single-impurity system.

The present results do not fully exhibit the expected rapid weakening of the "inelastic" (χ_{-+}^0) intensity with increasing T . Although the results for $T=15$ K do show this, the $T=50$ K results depart from this trend (except at small q). We attribute this disappointing

feature to several inadequacies of the present treatment:

(a) In the corresponding treatment for a single impurity,⁷ in the Kondo regime P_{lm} rises considerably higher than here (Fig. 1), with c_b thereby falling considerably lower. We expect an improved treatment to reflect this feature, as discussed in Sec. IV.

(b) As discussed above, the rapid decrease of the overall energy scale with increasing temperature is probably spurious. Keeping the inelastic peak at higher ω will reduce the amount of enhancement arising from the Bose factor.

(c) The intensity loss due to $c_b < 1$ is offset by some additional intensity proportional to P_{lm} . In the present approximation this is strictly elastic, i.e., proportional to $P_{lm}\delta(\omega)$, the result for noninteracting local moments. This is, of course, an oversimplification. In a higher-order treatment (the "two-parameter" version of I), there will be a Kondo-type interaction between the $\mathcal{E}_{k\sigma}^{\pm}$ quasiparticles and the unbound local moments, and this will broaden the P_{lm} contribution.⁴⁷ With the latter now adding to the "quasielastic" scattering, the *relative* strength of the χ_{-+}^0 contribution is decreased.

(d) The presence of unbound sites ($P_{lm} > 0$) will produce disordered-alloy-type broadening of the $\mathcal{E}_{k\sigma}^{\pm}$ spectrum. This must partially wash out the sharp structure, which is the phenomenological signature of the "inelastic" component.

Since all of these considerations tend to reduce the inelastic peak, or to make it less conspicuous, it seems very likely that a satisfactory theory will show the expected monotonic decrease of "inelastic" character with increasing T , for all q 's. Note also that point (c) implies a gradual replacement of "inelastic" character by "quasielastic" character, as indeed is seen experimentally.

The insulating-gap materials should be particularly favorable for observing the present "inelastic" features, because their "quasielastic" χ_{++}^0 contribution must vanish at $T=0$, and should remain small at $T < T_K$.³² The most studied of these materials is TmSe,³⁵ but unfortunately this has the additional complexity of two magnetic configurations and a magnetic ground state. [These features do not seem to alter the qualitative (q, ω) dependence significantly, however, according to Ref. 32.] Another obvious candidate, SmB₆, has the problem that natural Sm is unsuitable for neutron scattering.⁴⁸ This suggests that another insulating-gap material, YbB₁₂,⁴⁹ should be particularly interesting for detailed neutron study.

VI. RESISTIVITY

We shall briefly outline the implications of the present theoretical picture for resistivity. This discussion is intended to help clarify the concept of "coherence."

At $T=0$, the residual resistivity is due entirely to scattering of the $\mathcal{E}_{k\sigma}^{\pm}$ quasiparticles at the Fermi surface, by impurities and other lattice defects. There is now strong evidence that the T^2 term at $T \ll T_K$ is due to Baber scattering.^{23,50} In the present context this involves interactions between $\mathcal{E}_{k\sigma}^{\pm}$ quasiparticles in different subbands, with different effective masses. [Be-

sides a treatment of the quasiparticle interactions, this effect also requires generalization of the Hamiltonian (1) to include more than one "bare" conduction band ε_k , as discussed in I and Ref. 4.] This T^2 rise must, of course, saturate at some low T .

Before discussing the main contributions to the resistivity at higher T , we must note that although the present stage of approximation [based on (2)] does not involve either Kondo or spin-independent ("potential") scattering of conduction electrons (actually $\mathcal{E}_{k\sigma}^+$ quasiparticles) from local moments, both of these effects will enter at the next stage of our approximation scheme, the "two-parameter" version of I. We are therefore appealing, now, to this higher-order approximation.

A single active site contributes to scattering in several ways, depending on whether it is in a bound or unbound (local-moment) state. The bound-state scattering of a single site is very strong (near the unitarity limit), and can be characterized by a phase shift, but a perfect lattice of bound states produces only forward scattering. This totally coherent scattering generates the effective (quasiparticle) band structure, with its large effective mass enhancement. At finite temperature the absence of bound states on certain sites causes disordered-alloy-type scattering, with the unbound sites contributing via the "potential" (spin-independent) scattering. The CPA method is well suited for isolating the incoherent part of this scattering, but in applying this it is essential to properly treat the fully coherent $T=0$ situation,⁵¹ in contrast to the way CPA was used in Ref. 11. The resulting incoherent contribution must obviously be proportional to P_{lm} , at least when P_{lm} is fairly small. The remaining aspect is Kondo (spin-dependent and spin-flip) scattering from the unbound sites. Its resistivity contribution should have essentially the form $(a - b \ln T)P_{lm}$. To a fair approximation, then, the entire incoherent resistivity should have the same form $(a - b \ln T)P_{lm}$. For $T \lesssim T_K$ the resistivity must, therefore, rise steeply, closely following the initial rise of P_{lm} . The resistivity should then peak at a somewhat higher temperature than the peak of χ_{lm} , and it should then decay as $(a - b \ln T)P_{lm}$, i.e., more slowly than the decay of χ_{lm} . This picture will, of course, be modified at higher T by crystal-field excitations, which can sometimes (as for CeAl_3) produce the dominant peak in the resistivity.⁵²

As discussed in I, the band-theoretic resistivity due to $\mathcal{E}_{k\sigma}^+$ quasiparticles scattering off of defects should exhibit positive magnetoresistance, but as P_{lm} increases this will be overcome by the strong negative magnetoresistance due to spin-flip scattering. The sign change in magnetoresistance, which has been observed in several materials,³ is therefore easily understandable qualitatively.⁵³

VII. CONCLUDING REMARKS

We have presented a detailed treatment of the Anderson lattice at finite T . This work has identified the essential nature of the crossover mechanism, explaining this in terms of localized "moment-unbinding" excitations, and it has also shed light on low- T structures in the specific heat, magnetic susceptibility, and inelastic

neutron scattering. The previously vague notion of "coherence" is also clarified, as explained below and in Sec. VI. The present theoretical picture resembles phenomenological models in which local moments simply become unbound according to an activation-energy expression.^{13,14,54} In the present case, however, the activation energy $\zeta - \bar{\varepsilon}_f$ is temperature dependent, and it might even become strongly negative at $T > T_K$ in the Kondo-lattice or heavy-fermion regime. An improved treatment of $\mathcal{E}_{k\sigma}^+$ and $\bar{\varepsilon}_f$ is needed to clarify this aspect, and we hope to do this in future work. In part because of this present inadequacy, we have not attempted to precisely define the crossover temperature T_K .

The moment-unbinding excitations have clearly not been justified with the degree of rigor in, say, Luttinger's analysis,² but there is a variety of evidence which indicates that this concept is physically correct: (a) The Kondo-like ($a - b \ln T$) resistivity observed in many materials just above the resistivity peak temperature strongly suggests that the coherence [Eq. (15)] of the $\mathcal{E}_{k\sigma}^-$ excitations is destroyed by thermal agitation, as assumed in Sec. II. The sign change in magnetoresistance also supports this conclusion.^{3,53} (b) This concept is also supported by the remarkably strong T dependence of the "inelastic peak" seen in inelastic neutron scattering. [The mild experimental peaks or shoulders in C and (sometimes) in χ at $T \sim T_K$, referred to here as the "higher- T " features, are also consistent with this concept, but they do not necessarily rule out an explanation in terms of thermal $\mathcal{E}_{k\sigma}^-$ excitations.] (c) The moment-unbinding excitations require far less energy than $\mathcal{E}_{k\sigma}^-$ excitations, and are therefore strongly favored thermodynamically. (d) In the early stages of this investigation we made a concerted effort to explain the crossover in terms of $\mathcal{E}_{k\sigma}^-$ excitations alone, with due consideration of the "second refinement" described in Sec. II. (We had previously identified the $\mathcal{E}_{k\sigma}^-$ excitations as the underlying mechanism for the crossover.^{3,4}) This effort did not succeed. We found that reliance on "coherent" thermal $\mathcal{E}_{k\sigma}^-$ excitations tends strongly to produce a spurious second-order phase transition, in agreement with previous studies.⁶

With regard to the formal status of these localized excitations, we note that they are treated here by the same basic procedure used in I for the $\mathcal{E}_{k\sigma}^\pm$ excitations. We are directly implementing the formal quasiparticle recipe of Landau,¹⁸ $\mathcal{E}_{qp} = \delta \langle H \rangle / \delta f_{qp}$, where f_{qp} is a phenomenological occupation number. For each type of elementary excitation, we identify its f_{qp} with a suitable occupation number of the "uncorrelated" wave function $|\Phi_c \Phi_f\rangle$ in Eq. (2). The variational approach has provided the energies of the various assumed configurations, but, of course, it does not prove that the latter are eigenstates, or even reasonable approximations to eigenstates. At this stage, we can only appeal to the fact that the localized moment-unbinding excitations cost far less energy than any of the coherent $\mathcal{E}_{k\sigma}^-$ excitations. This major energy difference suggests that these localized excitations may be reasonable approximate eigenstates, in a sense similar to Landau quasiparticles, which generally have a finite lifetime. This aspect clearly deserves further study.

The single-impurity formalism, which the present theory most closely resembles, is known variously as the Lagrange-formula, Brillouin-Wigner, or self-consistent perturbation method.^{27,55} In contrast to these single-impurity studies, however, we renormalize only the bound state. The unbound (local moment) state is not allowed to hybridize until the next stage of refinement, the "two-parameter" version described in I. This feature avoids the problem of a spurious transition to a magnetic (unquenched local moment) ground state, which was encountered in these single-impurity studies when ε_f was moved from the mixed-valent to the Kondo regime. This feature emerges automatically from our approximation scheme, which is based on selecting a restricted set of single-site configurations, and then diagonalizing consistently within this set. For the lattice system, we expect that the next stage of refinement will generate the quasiparticle interactions of Fermi-liquid theory (here including the RKKY interaction), in addition to the "potential" (spin-independent) and Kondo (spin-dependent and spin-flip) interactions for each thermally unbound ion.

A hypothetical problem, which has received considerable attention recently,¹ is the suggestion that the Anderson lattice may not have enough conduction electrons available to screen away the moments of all N of the active sites.⁵⁶ This concern is unwarranted; in the present formalism the number of "screening" electrons is always precisely equal to the number of "bound" f^1 configurations.^{17,57}

The present picture is able to qualitatively explain many features of real materials, as shown here and in I: (a) The large effective mass m^* (large specific heat) at $T \ll T_K$. (b) The Luttinger features—Fermi surface or insulating gap. (c) The very-low-temperature peaks in C/T and χ , and the rapid drop in C/T at higher temperatures. (d) The rapid drop in resistivity as T is lowered below T_K . (e) The change of sign in magnetoresistance, at some $T^* < T_K$. (f) The unenhanced (by m^*) nature of ultrasonic attenuation and electron-spin-resonance relaxation, in the "normal" state below T_K . (g) "One-parameter" scaling of properties such as resistivity, under applied pressure, at temperatures low enough to avoid crystal-field excitations. (h) Some prominent features of inelastic neutron scattering.

In the present picture, there is just one dominant low-energy scale, T_K , determined by the $T=0$ value of

$(\xi - \bar{\varepsilon}_f)/k_B$. "Coherence" arises as the strong incoherent scattering by unquenched local moments is progressively frozen out, when T is lowered below T_K , thus there is no separate "coherence temperature" independent of T_K . Within the coherent regime, i.e., when $P_{lm} \ll 1$, physical properties become dominated by the renormalized-hybridization effective (quasiparticle) band structure. Physical properties, therefore, become sensitive to details such as the number and form of "bare" (ε_k) conduction bands intersecting the Fermi level, the band index and k dependence of the corresponding V_k 's, the crystal-field splitting, etc. We have speculated about some of the features to be expected from realistic hybridization band structures,^{3,4} such as the very-low-temperature peaks in C/T and χ seen above, but much remains to be done here.

The ubiquitous small exponential factor of Kondo theory enters here via the renormalization $\bar{V}_k^2/V_k^2 = 1 - \xi$,⁵⁸ at low T where $c_b \approx 1$. Since T_K itself is determined by features of the effective band structure, it follows that T_K and the scales of all other gap-related band features must be directly linked by geometrical factors.⁵⁹ The relation $m^* \sim (1 - \xi)^{-1}$ is just one example of this observation.⁶⁰ This is the explanation for the above statement that there is *only one* basic low- T energy scale, T_K , even though properties in the coherent regime are material-specific, depending on details of ε_k , V_k , and the crystal-field splitting. It follows that a *large* part of the low- T phenomenology, for any particular material, should simply scale with T_K . This is confirmed by the frequent phenomenological observation of "one-parameter" scaling, as in point (g) above.

Exceptions to this rule may arise from crystal-field excitations, from electrostatic (quadrupole-quadrupole) interactions, or from RKKY or quasiparticle interactions. RKKY coupling and/or interaction between quasiparticles are obviously essential for understanding certain properties (magnetism, superconductivity, $T^3 \ln T$ specific heat, and probably for the T^2 term in resistivity), but it is also important to recognize that much of valence-fluctuation physics can be understood, at least qualitatively, without considering these interactions.

ACKNOWLEDGMENT

This work was supported by the U.S. Department of Energy.

¹P. A. Lee, T. M. Rice, J. W. Serene, L. J. Sham, and J. W. Wilkins, *Comments Condens. Matter Phys.* **12**, 99 (1986).

²J. M. Luttinger, *Phys. Rev.* **119**, 1153 (1960).

³B. H. Brandow, *Phys. Rev. B* **33**, 215 (1986), referred to as I. This work was first reported at the Fourth International Conference on Valence Fluctuations, Cologne, 1984 [B. H. Brandow, *J. Magn. Magn. Mater.* **47-48**, 372 (1985)].

⁴See further discussion and references in B. H. Brandow, *J. Magn. Magn. Mater.* **52**, 25 (1985).

⁵T.-K. Lee and S. Chakravarty, *Phys. Rev. B* **22**, 3609 (1980), and references therein.

⁶P. Coleman, *J. Magn. Magn. Mater.* **47-48**, 323 (1985); *Phys.*

Rev. B **35**, 5072 (1987); Z. Tesanovic and O. T. Valls, *ibid.* **34**, 1918 (1986).

⁷B. H. Brandow (unpublished).

⁸A. Yoshimori and H. Kasai, *J. Magn. Magn. Mater.* **31-34**, 475 (1983); *Solid State Commun.* **58**, 259 (1986); M. Tachiki and S. Maekawa, *Phys. Rev. B* **29**, 2497 (1984); N. Grewe and T. Pruschke, *Z. Phys. B* **60**, 311 (1985).

⁹M. Matlack and W. Nolting, *Z. Phys. B* **55**, 103 (1984).

¹⁰B. H. Brandow, *Int. J. Quantum Chem. Symp.* **13**, 423 (1979).

¹¹H. J. Leder and G. Czycholl, *Z. Phys. B* **35**, 7 (1979); **38**, 219 (1980); G. Czycholl and H. J. Leder, *ibid.* **48**, 67 (1982); A. A. Aligia, J. Mazzafero, C. A. Balseiro, and B. Alascio, *J.*

- Magn. Magn. Mater. **40**, 61 (1983); A. A. Aligia and B. Alascio, *ibid.* **43**, 119 (1984); **46**, 321 (1985).
- ¹²N. Grewe, Solid State Commun. **50**, 19 (1984); T. Costi, J. Magn. Magn. Mater. **47-48**, 384 (1985); T. Koyama and M. Tachiki, Phys. Rev. B **36**, 437 (1987); Y. Kuramoto, C.-I. Kim, and T. Kasuya, Jpn. J. Appl. Phys. **26**, Suppl. 26-3, 459 (1987).
- ¹³E. E. Havinga, K. H. J. Buschow, and H. J. van Daal, Solid State Commun. **13**, 621 (1973).
- ¹⁴B. C. Sales and D. K. Wohlleben, Phys. Rev. Lett. **35**, 1240 (1975); B. C. Sales, J. Low Temp. Phys. **28**, 107 (1977).
- ¹⁵D. M. Newns and A. C. Hewson, J. Phys. F **10**, 2429 (1980); D. M. Newns, A. C. Hewson, J. W. Rasul, and N. Read, J. Appl. Phys. **53**, 7877 (1982).
- ¹⁶T. M. Rice, K. Ueda, H. R. Ott, and H. Rudigier, Phys. Rev. B **31**, 594 (1985).
- ¹⁷B. H. Brandow, J. Magn. Magn. Mater. **63-64**, 264 (1987).
- ¹⁸L. D. Landau, Zh. Eksp. Teor. Fiz. **30**, 1058 (1956) [Sov. Phys.—JETP **3**, 920 (1957)].
- ¹⁹N. Read and D. M. Newns, Solid State Commun. **52**, 993 (1984); T. M. Rice and K. Ueda, Phys. Rev. Lett. **55**, 995 (1985); **55**, 2093(E) (1985).
- ²⁰Specifically, we delete the k -dependent contribution of I, Sec. IV, and retain only the k -independent contribution μ , obtained in the Appendix.
- ²¹C. M. Varma and Y. Yafet, Phys. Rev. B **13**, 2950 (1976).
- ²²In a three-dimensional system the quasiparticle state density vanishes at the gap edge; thus a typical $\mathcal{E}_{k\sigma}$ excitation must have an energy somewhat beyond the gap edge.
- ²³K. Andres, J. E. Graebner, and H. R. Ott, Phys. Rev. Lett. **35**, 1779 (1975).
- ²⁴J. Aarts, F. R. de Boer, P. F. de Chatel, and A. Menovsky, Solid State Commun. **56**, 623 (1985).
- ²⁵H. Ludwigs, Ph.D. thesis, Universität Köln, 1981; D. Wohlleben (private communication).
- ²⁶P. de Chatel, Solid State Commun. **41**, 853 (1982).
- ²⁷T. V. Ramakrishnan and K. Sur, Phys. Rev. B **26**, 1798 (1982).
- ²⁸H. R. Krishna-murthy, K. G. Wilson, and J. W. Wilkins, Phys. Rev. Lett. **35**, 1101 (1975); in *Valence Instabilities and Related Narrow-Band Phenomena*, edited by R. D. Parks (Plenum, New York, 1977), p. 177; F. D. M. Haldane, Phys. Rev. Lett. **40**, 416 (1978).
- ²⁹A. J. Fedro and S. K. Sinha, in *Valence Fluctuations in Solids*, edited by L. M. Falicov, W. Hanke, and M. B. Maple (North-Holland, Amsterdam, 1981), p. 329; in *Moment Formation in Solids*, edited by W. J. L. Buyers (Plenum, New York, 1984), p. 135.
- ³⁰G. Czycholl and H. J. Leder, Z. Phys. B **48**, 67 (1982).
- ³¹D. L. Huber, Phys. Rev. B **28**, 860 (1983); **29**, 456 (1984); J. Appl. Phys. **55**, 1928 (1984).
- ³²A. A. Aligia and B. Alascio, J. Magn. Magn. Mater. **46**, 321 (1985).
- ³³A good discussion of these matrix-element factors may be found in R. P. Gupta and S. K. Sinha, Phys. Rev. B **3**, 2401 (1971).
- ³⁴(a) A real $4f$ ion with crystal-field (and spin-orbit) splitting has a Van Vleck term in its magnetic susceptibility. In the present context this contribution arises from the $q \rightarrow 0$ limit of the interband matrix-element factors when (i) the band states $\psi_{k\sigma}^{\pm}$ are obtained by hybridizing “bare” conduction bands with a set of crystal-field-split $4f$ ionic states on a lattice, and (ii) the correct magnetic matrix operator is used in place of e^{iqr} . See R. Kubo and Y. Obata, J. Phys. Soc. Jpn. **11**, 547 (1956); K. H. Oh, B. N. Harmon, S. H. Liu, and S. K. Sinha, Phys. Rev. B **14**, 1283 (1976), and references therein. There is no such orbital contribution for the present model, where the d and f orbitals have been replaced by s orbitals. (b) See Ref. 44.
- ³⁵M. Loewenhaupt and E. Holland-Moritz, J. Appl. Phys. **50**, 7456 (1979); E. Holland-Moritz, J. Magn. Magn. Mater. **38**, 253 (1983); B. H. Grier and S. M. Shapiro, in *Valence Fluctuations in Solids*, Ref. 29, p. 325; S. M. Shapiro and B. H. Grier, Phys. Rev. B **25**, 1457 (1982).
- ³⁶A. P. Murani, J. Phys. C **33**, 6359 (1983).
- ³⁷A. P. Murani, Phys. Rev. Lett. **54**, 1444 (1985).
- ³⁸R. M. Galera, D. Givord, J. Pierre, A. P. Murani, J. Schweizer, C. Vettier, and K. R. A. Ziebeck, J. Magn. Magn. Mater. **52**, 103 (1985); R. M. Galera, A. P. Murani, J. Pierre, and K. R. A. Ziebeck, *ibid.* **63-64**, 594 (1987).
- ³⁹G. Aeppli, H. Yoshizawa, Y. Endoh, E. Bucher, J. Hufnagel, Y. Onuki, and T. Komatsubara, Phys. Rev. Lett. **57**, 122 (1986).
- ⁴⁰G. Aeppli, A. Goldman, G. Shirane, E. Bucher, and M.-Ch. Lux-Steiner, Phys. Rev. Lett. **58**, 808 (1987).
- ⁴¹U. Walter, C.-K. Loong, M. Loewenhaupt, and W. Schlabitz, Phys. Rev. B **33**, 7875 (1986). See also C. Broholm, J. K. Kjems, W. J. L. Buyers, P. Matthews, T. T. M. Palstra, A. A. Menovsky, and J. A. Mydosh, Phys. Rev. Lett. **58**, 1467 (1987).
- ⁴²C. Broholm, J. K. Kjems, G. Aeppli, Z. Fisk, J. L. Smith, S. M. Shapiro, G. Shirane, and H. R. Ott, Phys. Rev. Lett. **58**, 917 (1987); **58**, 2003(E) (1987).
- ⁴³For a thorough discussion, see E. Holland-Moritz, D. Wohlleben, and M. Loewenhaupt, Phys. Rev. B **25**, 7482 (1982).
- ⁴⁴H. Shiba, J. Phys. Soc. Jpn. **55**, 2765 (1986). See especially Fig. 7.
- ⁴⁵T. A. Kaplan and S. D. Mahanti, Bull. Am. Phys. Soc. **17**, 292 (1972); and private communication. See also Eq. (3.6a) of Shiba, Ref. 44, for the case $u_k \rightarrow 1$, $v_k \rightarrow 0$.
- ⁴⁶A different correlation function has been calculated for the Hubbard Hamiltonian, again showing close agreement with the corresponding $U=0$ results: C. Gros, R. Joynt, and T. M. Rice, Phys. Rev. B **36**, 381 (1987).
- ⁴⁷K. W. Becker, P. Fulde, and J. Keller, Z. Phys. B **28**, 9 (1977); L. C. Lopes and B. Coqblin, Phys. Rev. B **33**, 1804 (1986).
- ⁴⁸E. Holland-Moritz, Physica (Utrecht) **136B**, 424 (1986).
- ⁴⁹M. Kasaya, F. Iga, M. Takigawa, and T. Kasuya, J. Magn. Magn. Mater. **47-48**, 429 (1985).
- ⁵⁰A. Auerbach and K. Levin, Phys. Rev. Lett. **57**, 877 (1986); K. Kadowaki and S. B. Woods, Solid State Commun. **58**, 507 (1986).
- ⁵¹A. Yoshimori and H. Kasai, Solid State Commun. **58**, 259 (1986). This point was also made by W. Wiethege, T. Costi, and P. Entel, Z. Phys. B **60**, 189 (1985).
- ⁵²K. H. J. Buschow, H. J. van Daal, F. E. Maranzana, and P. B. van Aken, Phys. Rev. B **3**, 1662 (1971); B. Cornut and B. Coqblin, *ibid.* **5**, 4541 (1972); Y. Lassailly, A. K. Bhattacharjee, and B. Coqblin, *ibid.* **31**, 7424 (1985).
- ⁵³This explanation for the sign change was first proposed by A. S. Edelstein, R. E. Majewski, and T. H. Blewett, in *Valence Instabilities and Related Narrow-Band Phenomena*, Ref. 29, p. 115.
- ⁵⁴The present picture of independent unbinding of sites has previously been proposed for the Anderson lattice, but with little justification and no consideration of low- T coherence

aspects: F. J. Ohkawa, J. Phys. Soc. Jpn. **52**, 3886 (1983). See also K. Ueda, *ibid.* **50**, 1162 (1981); **50**, 1173 (1981).
⁵⁵A. Bringer and H. Lustfeld, Z. Phys. B **28**, 213 (1977); P. Schlottmann, Phys. Rev. B **25**, 2371 (1982); F. C. Zhang and T. K. Lee, *ibid.* **28**, 33 (1983). In the present theory, the temperature dependence of the inelastic structure is essentially determined by this single-impurity picture, described by Schlottmann as promotion of an f electron into the conduction band. In contrast, the inelastic q and ω dependencies

are determined by the hybridization-gap aspect, which derives from the lattice periodicity.

⁵⁶P. Nozières, Ann. Phys. (Paris) **10**, 19 (1985).

⁵⁷Brandow, Ref. 3, beginning of p. 225.

⁵⁸Brandow, Ref. 3, see Eqs. (30) and (31).

⁵⁹Brandow, Ref. 3, see Eqs. (60)–(63).

⁶⁰Equation (56) of Ref. 3 contains a misprint. The correct form is $m^* \approx (W/2V)^2 \xi^2 / (1 - \xi)$.